Original Article
Repositioning antipsychotic fluphenazine hydrochloride for treating triple negative breast cancer with brain metastases and lung metastases

Fuyan Xu[1*], Yong Xia[1,2*], Zhanzhan Feng[1], Wentao Lin[3], Qiang Xue[1], Jinrui Jiang[4], Xi Yu[5], Cuiting Peng[1], Min Luo[6], Yufei Yang[1], Yuquan Wei[1], Luoting Yu[1]

[1]Department of Rehabilitation Medicine, State Key Laboratory of Biotherapy and Cancer Center, West China Hospital, Sichuan University and Collaborative Innovation Center for Biotherapy, Chengdu 610041, China; [2]Key Laboratory of Rehabilitation Medicine, West China Hospital, Sichuan University, Chengdu 610041, China; [3]Department of Plastic Surgery, The First Affiliated Hospital of Chongqing Medical University, Chongqing 400016, China; [4]West China School of Pharmacy, Sichuan University, Chengdu 610041, China; [5]Carey Bussiness School, Johns Hopkins University, Baltimore MD 21202, USA; [6]State Key Laboratory of Oral Diseases, National Clinical Research Center for Oral Diseases, West China Hospital of Stomatology, Sichuan University, Chengdu, Sichuan, China. *Equal contributors.

Abstract: Triple negative breast cancer (TNBC) patients have a high risk of brain metastases. This deadly disease represents a major challenge for successful treatment, in part because of the poor ability of drugs to penetrate the blood-brain barrier. Antipsychotic drugs show good bioavailability in the brain, and some of them have exhibited anticancer effects in several cancer types. In this study, we investigated the potential of repurposing fluphenazine hydrochloride (Flu) for the treatment of TNBC and the brain metastases. Our data showed that Flu inhibited survival of metastatic TNBC cells. It induced G0/G1 cell cycle arrest and promoted mitochondria-mediated intrinsic apoptosis *in vitro*. Pharmacokinetic studies in BALB/c mice showed a brain/plasma drug concentration ratio of Flu above 25 for at least 24 hours after dosing. Flu moderately suppressed tumor growth in a TNBC subcutaneous xenograft mouse model. Importantly, Flu exhibited good anti-metastatic potential in a mouse brain metastasis model with an inhibition rate of 85%. In addition, Flu showed a strong inhibitory effect on spontaneous lung metastasis. Moreover, Flu didn't cause serious side effects in the mice. Taken together, this study prompts further preclinical and clinical investigation into repurposing Flu for treating metastatic TNBC patients, which urgently need new treatment options.

Keywords: Fluphenazine, triple negative breast cancer (TNBC), brain metastasis, cell cycle arrest, apoptosis

Introduction

Breast cancer remains the most common type of cancer and the second leading cause of cancer-related mortality in females in the United States [1]. It is a heterogeneous disease with different histopathological features and therefore has different prognostic outcomes [2]. Among those, estrogen receptor (ER), progesterone receptor (PR) and human epidermal growth factor receptor-2 (HER2) 'triple negative' breast cancer (TNBC) is the most aggressive subtype with high risk of recurrence after conventional treatment [2, 3].

Metastasis results in approximately 90% of cancer mortality [4]. One of the biggest obsta-

cles in the treatment of breast cancer is the metastasis to other organs of the body, including the liver, bones, lungs and brain [5]. The incidence of brain metastases in TNBC patients can be as high as 46%, and the median survival after diagnosis is only 4.9 to 6.6 months [3, 6, 7]. Partly due to advanced imaging techniques and impressive treatment advances that prolong survival and better control systemic disease, the incidence of TNBC brain metastases has steadily increased over the years [5, 8]. Metastatic growth in the brain can lead to various neurological symptoms such as headache, cognitive impairment and motor dysfunction, which cause serious damage to the patient's quality of life [9, 10].

Sadly, the current treatment options for TNBC brain metastases are limited, only palliative, not curative. Patients with TNBC brain metastases are resistant to almost all existing treatments, including chemotherapy, surgical resection, stereotactic radiotherapy, and whole brain radiotherapy (WBRT) [11]. Therefore, the current situation underscores the urgent need to find better treatments to cure this terrible disease in the cerebral microenvironment.

Many chemotherapeutic drugs can't penetrate the blood-brain barrier (BBB), resulting in insufficient drug concentration in the brain lesion and therapeutic resistance to brain metastases [5, 12]. Thus, it's of great clinical significance to find new drugs that could enter the brain to treat brain metastases. Nowadays, the financial and time costs of anticancer drug development are increasing. However, the success rate is declining, making it more challenging to discover new anticancer drugs [13]. The strategy of drug repurposing has attracted great attention from both academics and pharmaceutical companies as an auxiliary process to tackle this challenge. It offers the opportunity to reuse drugs that have been approved for other disease indications, and to design new drug combinations or to change the formulation of the original drug [13-15]. In the field of oncology, lots of repurposing successes have proven the potential of this strategy, such as Aspirin (an antipyretic drug repurposed to treat colorectal cancer) and Metformin (an anti-diabetes drug repurposed to treat breast cancer, prostate cancer, et al.) [14, 16].

Published studies have shown an overall decreased cancer incidence in schizophrenic patients using neuroleptic drugs, implying that these drugs may have anticancer potentials [17, 18]. In addition, some anti-schizophrenia drugs, such as trifluoperazine and chlorpromazine, have shown anticancer efficacies in pre-clinical studies [19, 20]. Fluphenazine hydrochloride (Flu) is another commonly prescribed antipsychotic drug. Limited studies have reported its efficacy in the treatment of breast cancer, especially TNBC [21, 22]. As an anti-schizophrenia drug, Flu can penetrate BBB to reach a relatively high concentration in the brain. This prompted us to investigate its potential to treat TNBC and brain metastasis.

In this study, we evaluated the activity of Flu in the treatment of TNBC and brain metastases, and the possible underlying mechanisms. We also assessed its activity in suppressing lung, liver and bone metastases. We observed that Flu dramatically inhibited breast cancer cell growth and induced G0/G1 cell cycle arrest. It also induced mitochondria-mediated apoptosis in breast cancer cells. In addition, Flu inhibited migration and invasion of metastatic TNBC cells. Importantly, Flu treatment suppressed the growth of TNBC subcutaneous xenografts and brain metastases without causing serious side effects. Excitingly, we found Flu strongly impaired spontaneous lung metastasis of subcutaneous xenograft. Considering that Flu is an FDA-approved drug that can be rapidly entered into anti-cancer clinical trials, our findings support the possibility of repurposing Flu to treat TNBC with brain metastases and lung metastases, which lack effective treatment options.

Materials and methods

Materials

Fluphenazine hydrochloride (Flu) was purchased from AstaTech BioPharmaceutical Corporation (Chengdu, China). Flu was dissolved in DMSO/Cremophor EL/saline at 2.5:12.5:85 v/v for the *in vivo* experiments. MTT, DMSO, propidium iodide (PI), Rhodamine-123 (Rh123), Hoechst 33342 were purchased from Sigma. Annexin V-FITC/PI apoptosis detection kit, Annexin V-PE/7-AAD apoptosis detection kit and matrigel were purchased from BD Biosciences. The sources for the antibodies are shown in the supplementary materials (Table S1).

Cell lines and cell culture

Human TNBC cell line MDA-MB-231, mouse TNBC cell line 4T1 and other human breast cancer cell lines were purchased from the ATCC (American Type Culture Collection) within the past 5 years. The cells were cultured in DME/F-12 medium supplemented with 10% FBS, penicillin (100 U/ml) and streptomycin (0.1 mg/mL) under humidified condition with 5% CO_2 at 37°C.

MDA-MB-231 and 4T1 cells were authenticated via short tandem repeat (STR) analysis in 2018 by Shanghai Biowing Applied Biotechnology (SBWAB) Co. Ltd. Other cell lines were not further authenticated.

Cytotoxicity studies and colony formation assay

Cytotoxicity was determined as described previously with some modifications [23]. 2-5 × 10³ cells were seeded into 96-well plates and different concentrations of Flu was added to each well the next day. 20 µL MTT solution (5 mg/mL in saline) was added and incubated for 2 to 4 hours at 37°C after the indicated treatment time. 150 µL of DMSO was added to each well after removing the medium. The absorbance at 570 nm was read with a microplate spectrophotometer (Molecular Devices). IC$_{50}$ values were calculated with GraphPad Prism 5.

Colony formation assays were carried out as described previously with some modifications [24]. 4T1 cells or MDA-MB-231 cells were seeded in 6-well plates at 800 cells per well and treated by serial dilutions of Flu for 7-10 days. After terminating the assay, the colonies were stained with 0.5% crystal violet. Colonies (> 50 cells) were counted under an inverted microscope. Each assay was performed in three separate experiments. The survived clone of 4T1 and MDA-MB-231 cells were treated in 6-well plates for 30 days with indicated concentrations of Flu. Then the cells were cultured in 10 cm plate for another 10 days. Then cytotoxicity studies and clone-formation assay were done using those surviving cells. The proliferation curves of the surviving cells were carried out after seeding 1500-3000 cells in 96-well plates. Then cell numbers were measured by MTT as shown before for 5 consecutive days.

Cell and nuclei morphological analysis

After treatment with Flu for 48 hours, cells were washed with PBS and fixed in 4% paraformaldehyde followed by staining with Hoechst 33342 (10 µg/mL) for 30 min in the dark at room temperature. After washing with PBS, morphologies of the nuclei were analyzed with an inverted fluorescence microscope.

Cell cycle and apoptosis analysized by flow cytometry (FCM)

Cells were treated with Flu for 24 hours and fixed in ice old 75% ethanol. The fixed cells were incubated with 0.5 mL buffer containing 50 µg/mL PI and 0.1% Triton X-100 for 30 min. Cell cycle distribution was measured by ACEA

NovoCyte and analysed by NovoExpress software (ACEA Biosciences Inc., Hangzhou, China).

Apoptosis analysis was performed as previously described [25]. Briefly, cells were seeded at 1 × 10⁵ cells per well in 6-well plates and then treated with different concentrations of Flu for the indicated time. The levels of apoptosis were quantitatively examined by FCM using an Annexin V-FITC/PI or Annexin V-PE/7-AAD apoptosis detection kit. The data were analyzed by FlowJo or NovoExpress software. Each assay was replicated 3 times.

Measurement of mitochondrial membrane potential (ΔΨm) and ROS levels in cells

Rh123 was used to measure ΔΨm by FCM. After treatment with Flu for 24 hours, cells were incubated with Rh123 (5 µg/mL) for 30 min in the dark. Then, the cells were subjected to FCM.

DCFH-DA was used to measure ROS levels in the cells. Briefly, after treatment with Flu for 24 hours, cells were incubated with PBS containing 10 µM DCFH-DA for 30 min in the dark. After washing with PBS, cells were subjected to FCM.

Western blotting analysis

After treatment with Flu for 48 hours, cells were lysed in lysis buffer containing protease inhibitors Cocktail and PhosSTOP phosphatase inhibitors (Roche Diagnostics, UK) and sonicated on ice. Protein concentrations of the supernatant were measured with a BCA Protein Assay kit (Pierce, Rockford, IL, USA). Equal amounts of protein were subjected to SDS-PAGE gels and transferred onto PVDF membranes. After blocking with 5% nonfat milk in TBS/T, the membranes were incubated overnight with the relative primary at 4°C. After washing with TBS/T and incubation with the specific secondary antibodies conjugated to horseradish peroxidase, the protein bands were developed using an enhanced chemiluminescent substrate (Amersham, Piscataway, NJ). Quantification of the band intensities was based on three independent experiments using Image J software.

Scratch-induced migration assay in vitro

Scratch-induced wound healing assay was carried out as described previously with modifica-

tions [26]. When grow to 80% confluency in monolayer in 24-well plates, the cells were scratched by 10 μL pipette followed with treatment with 8 μM Flu. The wound width was measured 0 h, 18 h, 36 h and 48 h later by photography.

Tanswell migration and invasion analysis

Tanswell migration and invasion analysis were conducted as described previously with some modifications [24]. When performing transwell invasion aassay, boyden chamber (8 μm pore size) were coated with 50 μL diluted matrigel (PBS/matrigel = 4/1) and dried overnight under sterile conditions. 1 × 10⁵ 4T1 cells in serum-free medium were seeded in the top chamber and treated with 0.1% DMSO or indicated concentration of Flu. Then, 600 μL medium supplemented with 10% FBS containing equal amount of DMSO or Flu was added in the lower chamber. After 24 hours, the invaded cells were stained with 0.5% crystal violet and quantified.

Tanswell migration assay was conducted similarly to the above invasion assay with some modifications. The chamber was not precoated with 50 μL diluted matrigel. 5 × 10⁴ 4T1 cells in serum-free medium were seeded in the top chamber and treated with vehicle or indicated concentration of Flu. Then, 600 μL medium supplemented with 10% FBS containing equal amount of vehicle or Flu was added in the lower chamber. After treatment for 18 hours, migrated cells were stained and quantified.

Mouse pharmacokinetics studies

Pharmacokinetics studies were carried out as described previously with some modifications [27]. Flu was administered to naive female BALB/c mice by i.p. injection at 8 mg/kg, then blood and brain samples were collected at 1, 6, 12 and 24 hours post administration.

Flu was extracted from the plasma prepared from blood by protein precipitation using methyl alcohol containing internal standard (tolbutamide). The samples were centrifuged for 5 minutes at 14,000 rpm and 200 μL of the supernatant was subjected for UPLC/MS-MS analysis (Acquity UPLC, Waters; mass spectrometer, Applied Biosystems, TQ5500).

Brains were stored at -80°C after collecting. Following thawing, methanol/water (1:1 v/v)

mixture was added (1:10 brain: water w/v) and the samples were homogenized. The homogenate was centrifuged and subjected for UPLC/MS-MS analysis. The data were processed by Analyst software and the drug concentrations were calculated based on the standard curve.

Subcutaneous xenograft and intracarotid brain metastasis models

Subcutaneous xenografts were initiated by subcutaneous injection of 2.5×10^5 4T1 cells into right-flanks of eight-to-ten week old BALB/c mice (HFK Bioscience, Beijing, China). Flu treatment (8 mg/kg/day) via intraperitoneal injection (i.p.) was started when the tumor volume reached approximately 100 mm³. The tumor size and body weight of the mice were measured every 3 or 4 days. The tumor volumes were calculated according to the following equation: volume = 3.14 × length (mm) × width (mm)²/6.

Brain metastasis model was established by intracarotid injection as described previously with some modifications [28]. Briefly, 5×10^4 luciferase-expressing 4T1 cells in 100 μL sterile HBSS were injected into the right common carotid artery of the mice. After formation of severe metastases, the brains of the mice were isolated and minced by using cell strainer with pore size of 70 μm (BD Biosciences). About 10 days later, expanded 4T1 cells on the tissue culture dish were collected as brain-seeking sublines (4T1 Br1-pluc). For drug treatment assays, 1×10^4 4T1 Br1-pluc cells were injected into the right common carotid artery of the mice. Metastasis growth in the brain was monitored by non-invasive *In Vivo* Imaging System (IVIS, PerkinElmer) every 3 or 4 days. Flu was administered at 8 mg/kg by i.p. injection once daily three or eight days after the inoculation. At the end of experiments, the brains were dissected to measure the luciferase signal in the isolated brains.

Establishment of lung metastasis, liver metastasis and bone metastasis models

4T1 cells are easily to form spontaneous lung metastasis in BALB/C mice. Lungs were harvested in the subcutaneous xenograft model after the mice were killed by rising CO_2. Then the total number of lung metastases was counted by naked eyes [29].
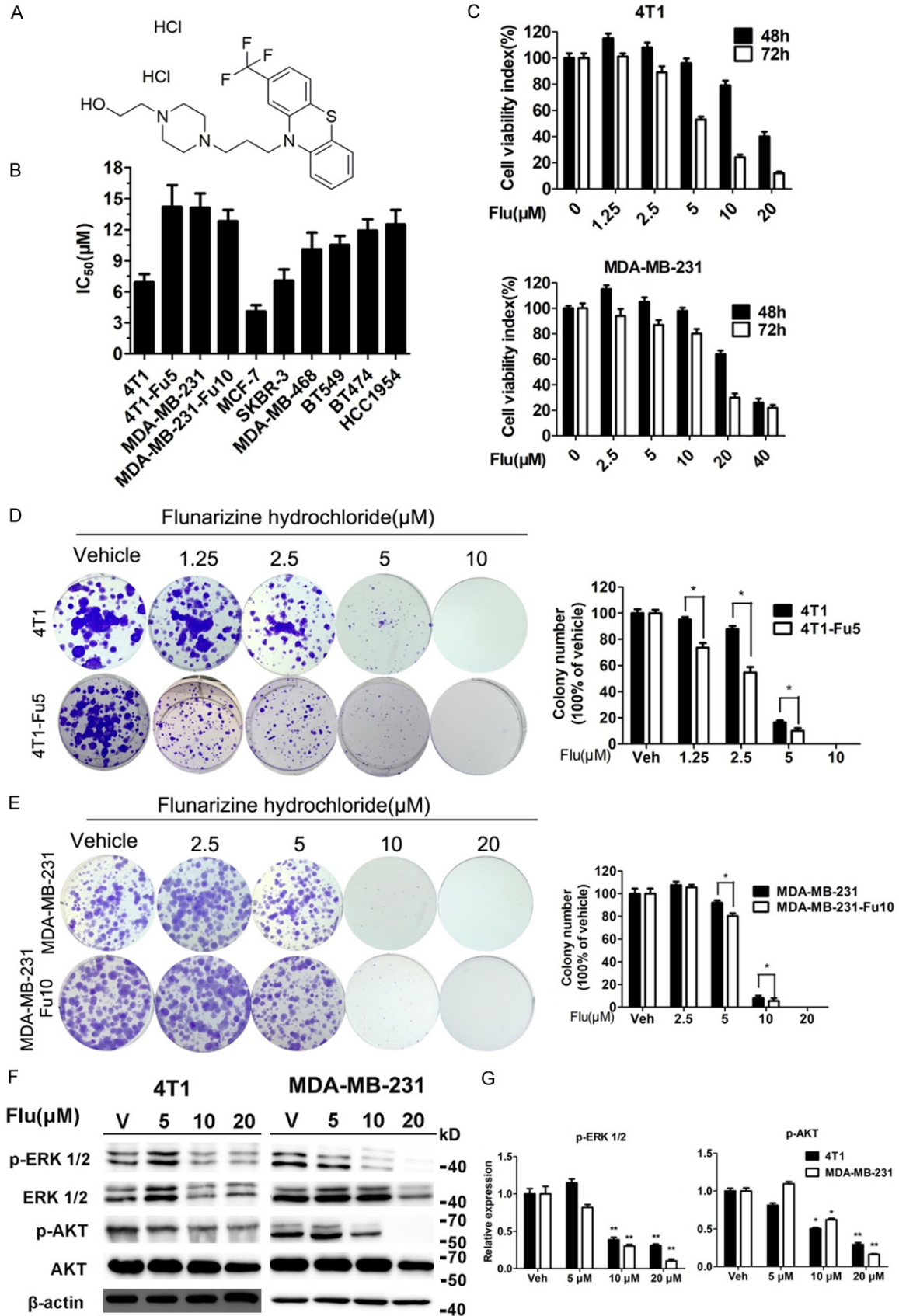
Figure 1. Flu inhibited viabilities of breast cancer cell lines. A. Chemical structure of Flu. B. Inhibitory effects of Flu on the viabilities of several breast cancer cell lines after 72 hours of treatment (IC_{50} values, μM). C. Dose- and concentration-dependent inhibitory effects of Flu on cell viabilities in two TNBC cell lines (4T1 and MDA-MB-231). MTT assays were used to measure cell viabilities after Flu treatment for 48 and 72 hours, respectively. Viabilities of vehicle treated cells at each time point were counted as 100%. D and E. Inhibitory effects of Flu on 4T1, 4T1-Fu5, MDA-MB-231 and MDA-MB-231-Fu10 cell colony formation. Quantifications are shown in the right for each cell line. Images shown are representatives from three independent experiments. F. Flu treatment decreased phosphorylation of ERK1/2 and AKT in 4T1 and MDA-MB-231 cell lines. Molecular weight of bands on Markers are shown on the right of each image (kilo Dalton, kD). β-actin served as the internal control. Images shown are representatives from three independent experiments. G. Relative expression of phosphorylation of ERK1/2 and AKT were quantified using Image J software and normalized to β-actin expression. *P<0.05; **P<0.01; ***P<0.001.

Liver metastasis model was established based on the method reported below with some modifications [30]. Briefly, 25×10^4 luciferase-expressing 4T1 cells in 25 μL sterile HBSS were injected into the tip of the spleen between 30 to 60 s. Then we placed a cotton ball for 3 minutes on the injection site and closed the flank incision in two layers. Three days after the injection, the mice were divided into vehicle and Flu treatment groups. The growth of the liver metastasis was monitored by IVIS every week.

Bone metastasis was established as described previously with some modifications [31]. Briefly, 2.5×10^4 luciferase-expressing 4T1 cells in 10 μL sterile HBSS were injected into the tibial growth plate on the back left leg. Flu treatment started three days after the inoculation. The growth of the bone metastasis was monitored by IVIS every week.

Immunohistological analysis of tumor sections

The IHC analysis of tumor tissues was carried out as described by us and others with modifications [32, 33]. Tumor tissues from the mice were obtained and fixed at the end of the treatment. The fixed tumors were sectioned into 5 μm thick sections on the slides after dehydrating and embeding in paraffin. The sections were then deparaffinized, rehydrated. After antigens retrieval, the sections were incubated with 3% H_2O_2 solution and blocked with 5% goat serum, followed by incubating with the specific antibodies for cleaved casapase 3 and Ki67 overnight at 4°C. The slides were stained using a DAB detection kit.

Toxicity evaluation

The mice were monitored every day to assess the side effects and toxicities during Flu treatment. The mice were euthanized on the 17th day of treatment and the eyeball blood was collected. Hematological and serum biochemistry analysis were performed using the eyeball blood. Major organs including heart, liver, kidney and brain were stained with H&E for histopathologic examination.

Statistical analysis

Data were represented as means ± SD from three independent experiments and analyzed by GraphPad Prism 5. Statistical significance was analyzed using two-tailed Student t tests. Statistically significant *P*-values were expressed as follows: *P<0.05; **P<0.01; ***P<0.001.

Results

Flu suppressed proliferation of breast cancer cells

To investigate the effects of Flu on the viability of breast cancer cells, 8 breast cancer cell lines were exposed to Flu. Flu reduced their survival with IC_{50} values less than 15 μM (**Figure 1B**). We are interested in finding new drugs to treat TNBC. Thus, we chose human TNBC cell line MDA-MB-231 and mouse TNBC cell line 4T1 for further experiments. As shown in **Figure 1C**, Flu inhibited TNBC cell viabilities in a time-dependent as well as concentration-dependent manner.

Flu inhibited TNBC cell growth/survival assessed by colony formation assay

We performed colony formation assay to visually assess the inhibitory activity of Flu on proliferation/survival of 4T1 and MDA-MB-231 cells. Clearly, Flu significantly inhibited the number and size of TNBC cell colonies (**Figure 1D** and **1E**). No cells survived under 10 and 20 μM Flu treatment in 4T1 and MDA-MB-231, respectively. We also treated 4T1 and MDA-MB-231 cells with Flu at 5 and 10 μM for 30

days and assessed the inhibition of Flu on those surviving cells (labeled as 4T1-Fu5 and MDA-MB-231-Fu10 cells, respectively). The surviving 4T1 cells were slightly resistant to Flu and the IC_{50} value increased from 6.9 to 14.20 µM after 72 hours of Flu treatment (**Figure 1B**). However, the proliferation rate of 4T1-Fu5 cells was slower than the parental cells (Figure S1). Flu strongly inhibited the colony formation abilities of 4T1-Fu5 (**Figure 1D**). There were no significant differences between the parental cells and resistant cells when comparing the IC_{50} after Flu treatment for 72 hours (**Figure 1B**), the proliferation rate (Figure S1) and the inhibitory effects of Flu on colony formation (**Figure 1D**) for MDA-MB-231 cells.

Flu decreased the expression of p44/42 ERK and phosphorylated AKT, two key molecules in RAS/RAF/MEK/ERK and PI3K-AKT-mTOR pathway, in both TNBC cell lines, suggesting that inhibiting these two pathways contributed to the inhibition of TNBC cell growth/survival (**Figure 1F** and **1G**).

Flu induced G0/G1 phase arrest in TNBC cells

To investigate the molecular mechanisms underlying the inhibitory effects of Flu on TNBC cells, we assessed whether Flu regulated cell cycle by FCM. Clearly, 24 hours of Flu treatment induced significant G0/G1 phase arrest concentration dependently in both cell lines (**Figure 2A**, **2B**, **2E**, **2F**). The G0/G1 phase distribution was increased from 36.3% in vehicle treat group to 45.2% after 20 µM Flu treatment in 4T1 cells. Similar results were seen in MDA-MB-231 cells. These data implied that G0/G1 phase arrest contributed to the anticancer effect of Flu.

We next extended the investigation to the expression levels of some critical proteins involved in G0/G1 phase regulation. The data showed that Flu down-regulated the expression levels of cyclin-dependent kinase (CDK) 2, CDK4, cyclin D1, and cyclin E in a concentration-dependent manner (**Figure 2C**, **2D**, **2G**, **2H**). p21 and p27 have important roles in G1/S cell cycle transition. In our experiments, Flu upregulated the expression of p21 in both cell lines. Meanwhile, the level of p27 was increased after Flu treatment in MDA-MB-231 cells.

Flu induced apoptosis of TNBC cells

We next assessed whether Flu treatment induced TNBC cell apoptosis to exert the anticancer effects. After treatment with Flu for 48 hours, both TNBC cell lines showed cell shrinkage, a typical feature of apoptotic cells (**Figure 3A**). Hoechst 33342 staining assay further confirmed that Flu altered the cells' nuclei morphology after 48 hours treatment, as indicated by the nuclear fragmentation, reduction cell volume and formation of condensed nuclei with bright-blue fluoresce (**Figure 3B**).

We also used FCM to quantitatively measure the apoptosis after Annexin V-FITC/PI staining. The data showed Flu significantly induced TNBC cell apoptosis (**Figure 3C**). The proportion of apoptotic 4T1 cells dramatically increased from 4.3% to 86% when the concentration of Flu increased from 0 to 20 µM after 72 hours of treatment. Similar results were seen in MDA-MB-231 cells. Protein expression analysis of some key proteins also indicated the apoptosis. Flu treatment increased the cleavage of caspase 3 in both cell lines (**Figure 3D** and **3E**). These findings revealed that induction of apoptosis contributed to Flu's inhibiting activities toward TNBC.

Flu likely induced apoptosis via the intrinsic apoptosis pathway

To further elucidate the mechanisms of the apoptosis, the expression levels of some apoptosis-related proteins were detected. As indicated in **Figure 3D** and **3E**, Flu treatment resulted in decreased expression of Bcl-2 in both cell lines. The expression of Bax is slightly increased after Flu treatment in MDA-MB-231 cells. These findings suggested that Flu might induce apoptosis via the mitochondria-mediated intrinsic apoptotic pathway. To verify this hypothesis, we measured the changes in ΔΨm after Flu treatment by FCM using the green dye Rh123. The data showed that Flu led to ΔΨm loss in both cell lines (**Figure 4A** and **4B**).

Cancer cells are under oxidative stress partially due to the uncontrolled proliferation and other defects. ROS is mainly generated in mitochondria and its accumulation in cancer cells could lead to cell death if the normal redox signal pathway is disrupted. In the study, we detected ROS levels in the cells using the dye DCFH-DA.
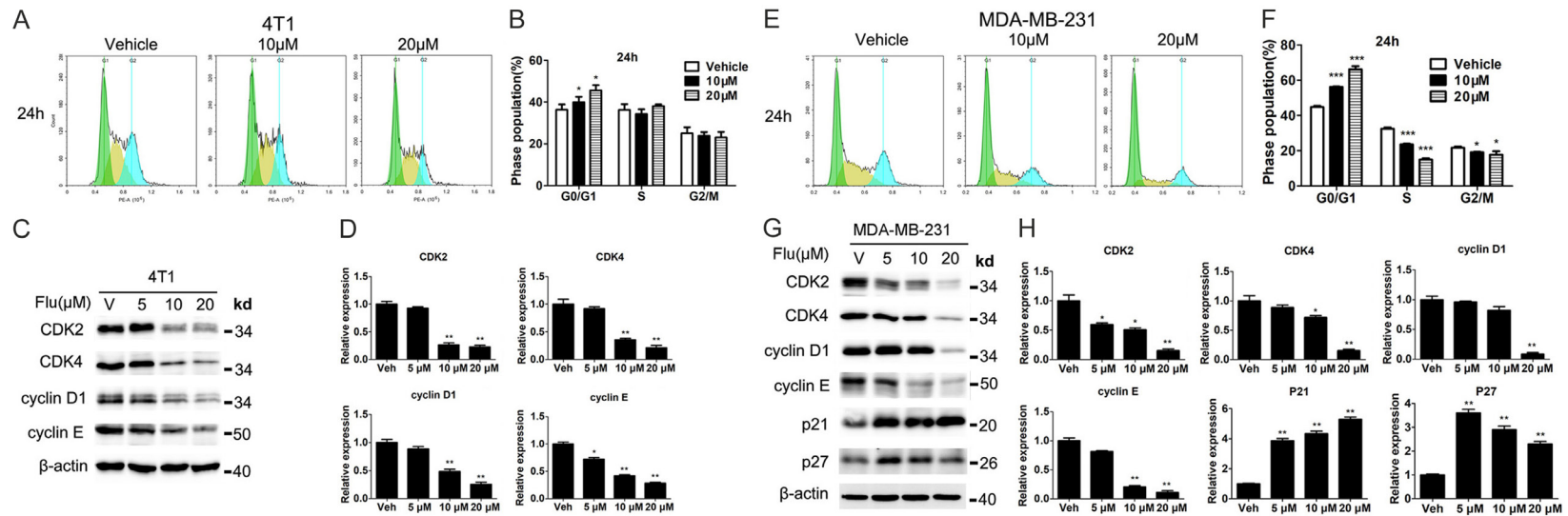
Figure 2. Flu induced G0/G1 arrest in 4T1 and MDA-MB-231 cells. (A and E) 4T1 and MDA-MB-231 cells were treated with 0.1% DMSO and indicated concentrations of Flu for 24 hours. The cells were then incubated with 50 µg/mL PI and analyzed by FCM. Images shown are representative from three independent experiments. (B and F) Quantified histograms of cell cycle distributions after Flu treatment for 24 hours in 4T1 and MDA-MB-231 cells. (C and G) Effects of Flu on the expressions of proteins related in G0/G1 regulation. The expressions of CDK2, CDK4, cyclin E, cyclin D1, p21 and p27 after Flu treatment for 24 hours at indicated concentrations are shown. Molecular weight of bands are shown to the right of each image (kilo Dalton, kD). β-actin served as the internal control. Images shown are representatives from three independent experiments. (D and H) Protein expressions from (C and G) were quantified using Image J and normalized to β-actin expression. *P<0.05; **P<0.01; ***P<0.001.
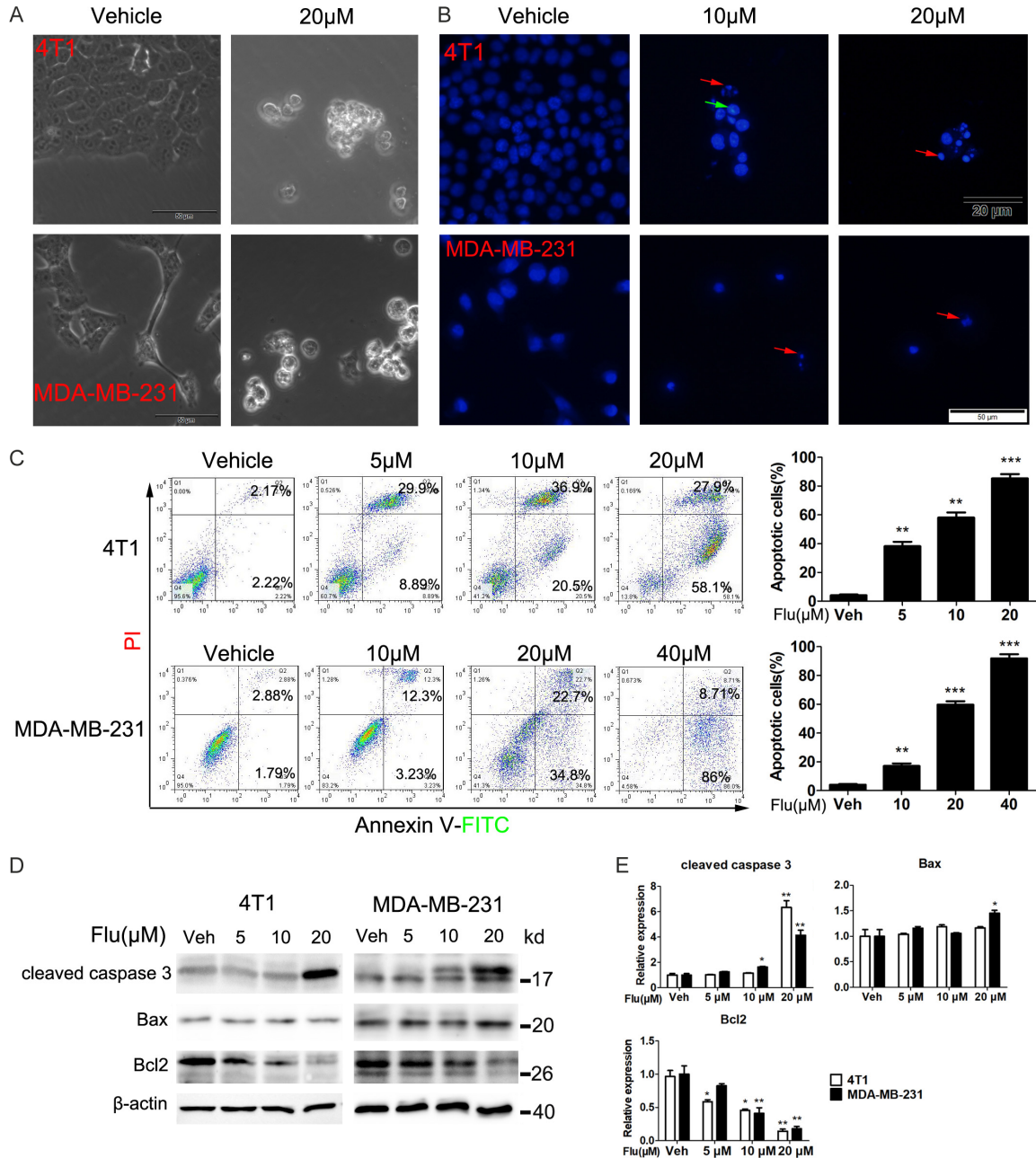
Figure 3. Flu induced apoptosis in 4T1 and MDA-MB-231 cells. (A and B) Effects of Flu on the morphology of 4T1 and MDA-MB-231 cells. (A) The cells were treated with 20 μM Flu for 48 hours. Then, bright-field microscope images of the cells were taken. The scale bars represent 50 μm. (B) Cancer cell nuclear alterations after Flu treatment for 48 hours. 4T1 and MDA-MB-231 cells were treated with indicated concentrations of Flu or vehicle for 48 hours. Then, the cells were stained with Hoechst 33258 and analyzed by fluorescence microscope. The red and green arrows indicated nuclear fragmentation and condensed nuclei, respectively. The scale bars represent 20 μm and 50 μm for 4T1 and MDA-MB-231 cells, respectively. (C) The apoptosis of 4T1 and MDA-MB-231 cells after Flu treatment were quantitatively analyzed by FCM. Cells were treated with indicated concentrations of Flu or vehicle for 72 hours and then labeled with AnnexinV-FITC and PI followed by FCM analysis. Images shown are representatives of three independent experiments. Quantified values are shown to the right of each cell line. (D) Expression levels of key apoptosis-related proteins were detected by western blotting. Cells were treated with vehicle or indicated concentrations of Flu for 72 hours. Then, the expression levels of cleaved caspase-3 and Bcl-2 family proteins were determined. Images presented are representatives of three independent experiments. (E) Expressions of the protein were quantified using Image J and normalized against β-actin expression. *P<0.05; **P<0.01; ***P<0.001.
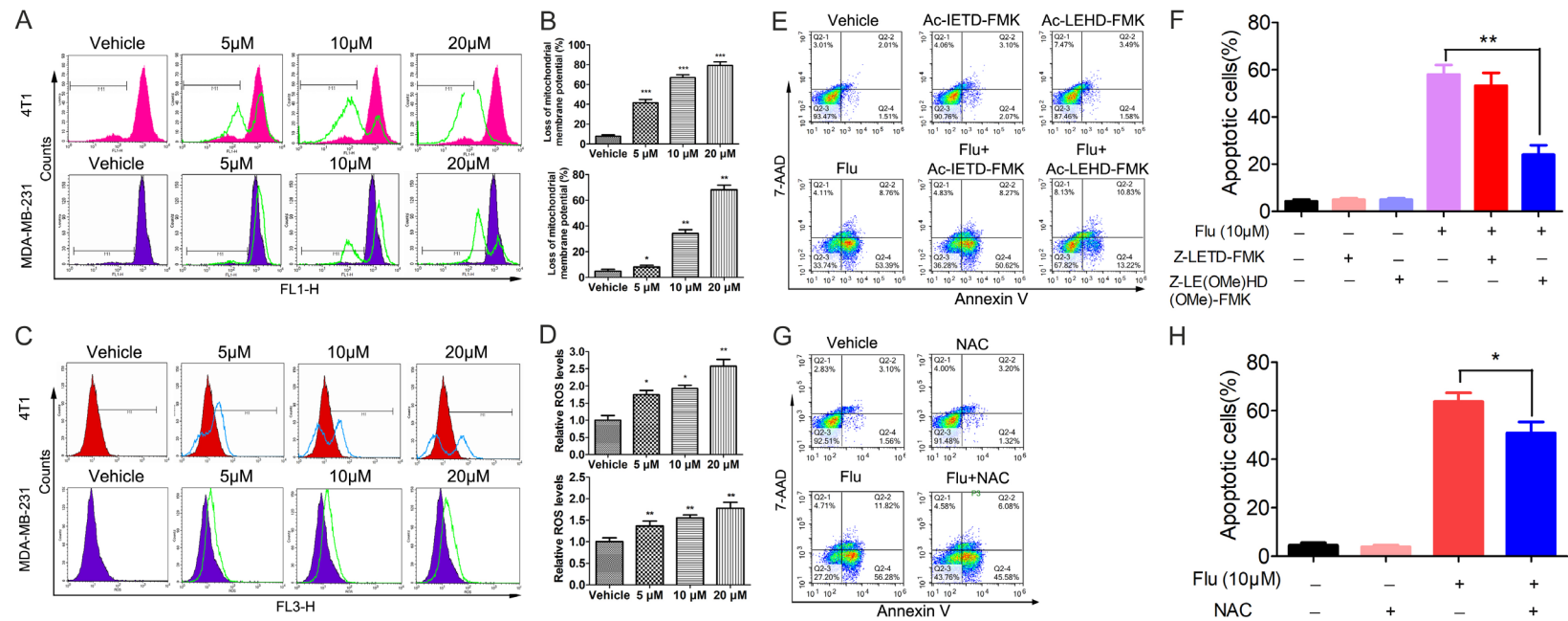
Figure 4. Effects of Flu on the intrinsic apoptosis pathway. (A and B) Flu decreased the ΔΨm in TNBC cancer cells. 4T1 and MDA-MB-231 cells were treated with vehicle or indicated concentrations of Flu for 24 hours and then stained with Rh123 to measure the changes of ΔΨm by FCM. (A) Images shown are representative of three independent experiments. (B) Quantified results are shown on the right. (C and D) Flu treatment increased ROS levels in TNBC cancer cells. After treatment with indicated concentrations of Flu for 12 hours, 4T1 and MDA-MB-231 cells were incubated with 10 μM DCFH-DA. Intracellular ROS levels were then measured as DCF fluorescence by FCM. (C) Images shown are representative of three independent experiments. (D) Quantified results are shown on the right. (E and F) 4T1 cells were treated with 10 μM Flu alone or in combination with Z-LE(OMe)HD(OMe)-FMK (caspase-9 inhibitor) or in combination with Z-LETD-FMK (caspase-8 inhibitor) for 72 hours. Then the apoptosis of the cells was measured by FCM after AnnexinV-PE and 7-AAD labeling. (E) Images shown are representatives of three independent experiments. (F) Quantified values are shown on the right. (G and H) 4T1 cells were pretreated with 2 mM NAC for 1 h and then treated with 10 μM Flu for 72 hours. The apoptosis of the cells was measured after AnnexinV-PE and 7-AAD labeling. (G) Images shown are representatives of three independent experiments. (H) Quantified values are shown on the right. *P<0.05; **P<0.01, ***P<0.001.

Obviously, the amount of ROS in both cell lines increased significantly after Flu treatment for 12 hours (**Figure 4C** and **4D**).

We also used some caspase inhibitors and the antioxidant NAC to investigate whether Flu-induced apoptosis is specifically associated with caspase activation and to evaluate which type of apoptosis is predominant. The data showed that Z-LE(OMe)HD(OMe)-FMK (caspase-9 inhibitor) could partially reverse Flu-induced apoptosis, while Z-LETD-FMK (caspase-8 inhibitor) showed weaker effects (**Figures 4E**, **4F**, S2A and S2B). Meanwhile, the antioxidant NAC could rescue the extent of Flu-induced apoptosis (**Figures 4G**, **4H**, S2C and S2D). The above data indicated that the mito-chondria-mediated intrinsic pathway played a more important role in Flu-induced apoptosis than the extrinsic pathway.

Flu inhibited TNBC xenograft growth in BALB/c mice

BALB/c mice bearing 4T1 subcutaneous xenograft were administered with Flu by i.p. injection at 4 and 8 mg·kg^{-1}·day^{-1}. Flu moderately suppressed tumour growth in a dose-dependent manner and the tumour growth inhibition rate at day 17 postinoculation is about 48% in 8 mg/kg treatment group (**Figure 5A**).

Moreover, immunohistochemistry analyses of the tumor tissues were conducted to elucidate the anti-tumor mechanism. Indeed, Flu treatment suppressed cancer cell proliferation in the tumor sections as indicated by decreased Ki67 staining (**Figure 5C**). Besides, cleaved caspase-3 staining told that Flu treatment induced cancer cell apoptosis *in vivo* (**Figure 5D**).

Flu suppressed TNBC cell migration and invasion in vitro

Migration and invasion are pivotal steps in the cancer metastasis process. Therefore, we used wound healing assay and transwell assay to evaluate the effects of Flu on TNBC cell migration and invasion. As shown in Figure S3A, Flu dramatically suppressed the wound healing course. Similar results were observed in transwell migration assays (Figure S3B). Furthermore, transwell invasion assays indicated that Flu treatment significantly suppressed the inva-

sion of 4T1 cells through the matrigel and barrier (Figure S3C). The above data suggested that Flu suppressed TNBC cell migration and invasion in vitro, prompting us to investigate its in vivo activities to inhibit metastasis.

Flu suppressed brain metastasis of 4T1 cells in vivo

Firstly, we investigated the drug concentration of Flu in the plasma and brain after i.p. injection. Strikingly, Flu was highly distributed in brain after a single dose of 8 mg/kg (**Figure 6A**). The brain/plasma drug concentration ratio was above 25 for at least 24 hours after the drug administration. Then we validated the *in vivo* anti-metastasis efficacy of Flu in an experimental breast cancer brain metastatic model. Based on the luminescence intensity, it's obvious that Flu treatment significantly suppressed the metastasis growth in the brain when the treatment started on day 3 after establishing the brain metastasis model (**Figure 6B** and **6C**). Quantification of the luminescence intensity indicated an inhibition rate of 85% on the brain metastasis growth by Flu treatment. The luminescence signal in the removed brain confirmed the success of establishing brain metastasis model. The data showed that the brain metastasis was suppressed by 75% after Flu treatment (**Figure 6D** and **6E**). Notably, Flu also significantly suppressed brain metastasis from 4T1 cells even if the treatment started on day 8 after establishing the brain metastasis model (**Figure 6G** and **6H**).

Flu suppressed spontaneous lung metastasis of 4T1 cells in vivo

We counted the number of visible metastasis in the lungs after terminating the treatment of 4T1 xenograft. Excitingly, Flu also showed strong inhibition on spontaneous lung metastasis with an inhibition rate of 76% at 8 mg/kg (**Figure 7A** and **7B**). However, Flu didn't suppress experimental bone and liver metastasis in our studies (**Figure 7C-F**).

Flu didn't induce obvious side effects in the mice during the treatment

The above data conclusively showed that Flu had the potential to be a new drug for treating metastatic TNBC. Efficacy and safety profiles are two key features of a successful anti-can-
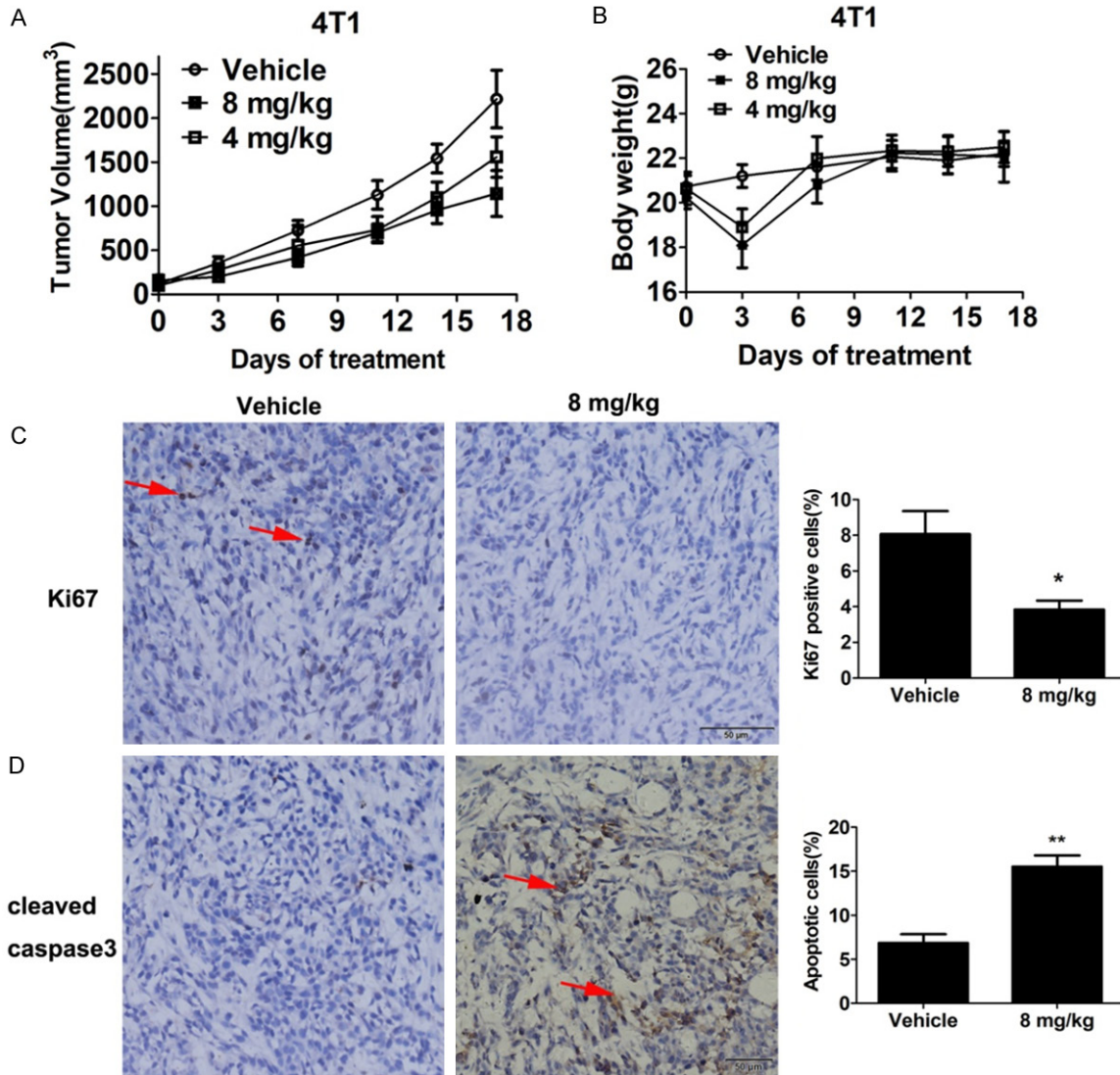
Figure 5. Anti-tumor effects of Flu in 4T1 subcutaneous tumor model. 25 × 10⁴ 4T1 cells were injected subcutaneously in female BALB/c mice. Flu administration was started when the average tumor volume reached to about 100 mm³. Vehicle or Flu was administered by i.p. every day. Tumor diameters and body weights of the mice were measured every 3 or 4 days. Data are expressed as means ± SD (n = 7). A. Tumor size changes in mice during Flu treatment. B. Body weights changes of the mice during Flu treatment. C and D. Tumors from each group were fixed in formalin overnight and processed for paraffin embedding after 10 days treatment, followed by IHC analysis. Then, the tumor tissues were sectioned and immunostained for proliferation (Ki67) and apoptosis markers (cleaved caspase 3). C. 8 mg/kg Flu treatment decreased the proportion of Ki67 positive cells as indicated by the arrow. Quantified results are shown on the right. D. Flu treatment increased the proportion of cleaved-caspase-3 positive cells in the tumor tissue as indicated by the arrow. Quantified result is shown on the right. *P<0.05, **P<0.01.

cer drug. Then we assessed whether Flu caused any serious side effects or toxicity.

During the treatment of 4T1 xenograft, we did not observe serious side effects and toxicities after Flu treatment. Although there was a body weight loss at day 3 after the treatment, it's reversible. The mice recovered from the weight

loss after that day and they have comparable weight with the mice from the vehicle treatment group (**Figure 5B** and data not shown). Notably, we didn't observe weight loss during the treatment of 4T1 brain metastasis model in BALB/c mice (**Figure 6F**). Although extrapyramidal side effect (EPS) was shown in several cases, it disappeared rapidly within a few minutes. Fur-
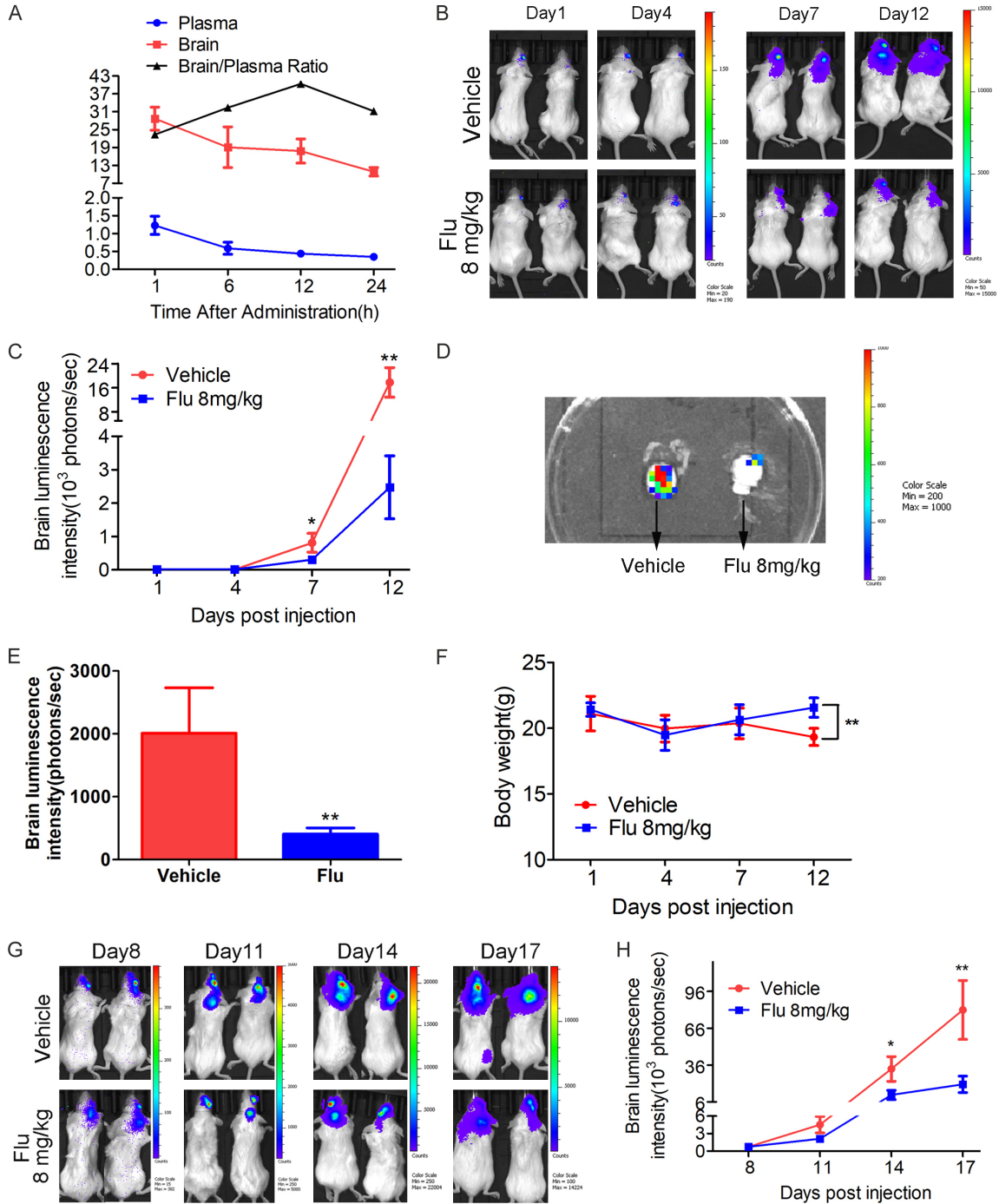
Figure 6. Pharmacokinetic studies of Flu and its activities to inhibit TNBC brain metastasis growth in the mice. A. Flu highly penetrated to the brain. Flu was dosed at 8 mg/kg to naive female BALB/c mice by i.p. injection and then heart blood and brain samples were collected at 1, 6, 12 and 24 hours postdose. Drug concentrations in the plasma and brain were measured via UPLC/MS-MS analysis (n = 3). The unit for plasma drug concentration, brain drug concentration and brain/plasma ratio are µM/L, µM/kg and L/kg. B-F. 1×10^4 4T1 Br-luc breast cancer cells were injected in into the right common carotid artery of mouse to establish brain metastasis model. The mice were treated with 8 mg/kg of Flu via i.p. injection 3 days postinoculation. The growth of the metastasis in the brain was monitored via IVIS every 3 or 4 days. B. Representative luminescence images of the mice in each group at the indicated time. The exposure time for day 1, day 4, day 7 and day 12 is 180 seconds, 180 seconds, 60 seconds and 10 seconds, respectively. C. Brain luminescence intensity change during the treatment (n = 11). D and E. The brain of each mouse was isolated after terminating the treatment. Then luminescence images of the brain were plotted. D. Representative luminescence image of the isolated brain from vehicle and Flu treatment group. E. Quantified

luminescence intensity of the isolated brain (n = 11). F. Body weight changes of brain metastasis-bearing mice during the treatment. G and H. Effects of Flu on brain metastasis growth when the treatment started on day 8 post-inoculation. 1 × 10^4 4T1 Br-luc cells were injected to establish brain metastasis model. The mice were treated with 8 mg/kg of Flu by i.p. injection 8 days postinoculation. G. Representative luminescence images of the mice at the indicated time. The exposure time for day 8, day 11, day 14 and day 17 is 60 seconds, 60 seconds, 30 seconds and 10 seconds, respectively. H. Brain luminescence intensity changes during the treatment (n = 10).
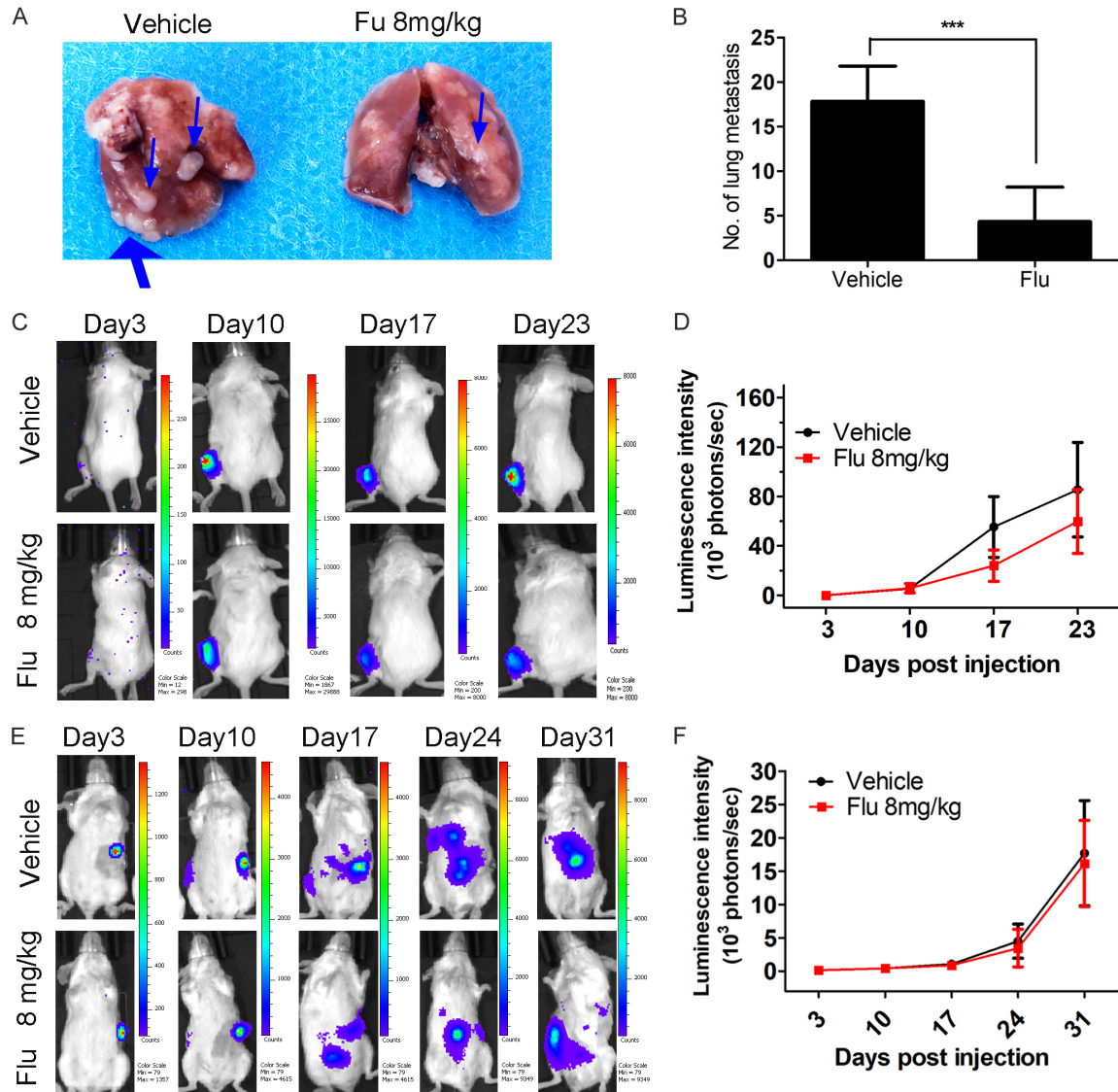
Figure 7. Effects of Flu on lung metastasis, liver metastasis and bone metastasis in mouse models. A and B. Flu strongly inhibited spontaneous lung metastasis. Lungs were harvested in the subcutaneous xenograft model. Then the total numbers of lung metastases were counted with eyes. A. Blue arrows indicate the metastasis on the surface of the lung. B. Quantified values were shown in the right. ***P<0.001. C and D. Flu didn't inhibit the growth of bone metastasis. 2.5 × 10^4 luciferase-expressing 4T1 cells in 10 μL sterile HBSS were injected into the tibial growth plate on the back left leg to establish experimental liver metastasis model. The growth of bone metastasis was measured via IVIS every week. E and F. Flu didn't show inhibition on liver metastasis. 25 × 10^4 luciferase-expressing 4T1 cells in 25 μL sterile HBSS were injected into the tip of the exposed spleen to establish experimental liver metastasis model. Then the growth of liver metastasis was measured via IVIS every week.

thermore, after 17 days of treatment, Flu didn't cause significant changes of hematological and serum biochemical parameters in the BALB/c mice (**Figure 8A** and **8B**). Histological examinations of heart, liver, kidney and brain as assessed by H&E staining neither showed
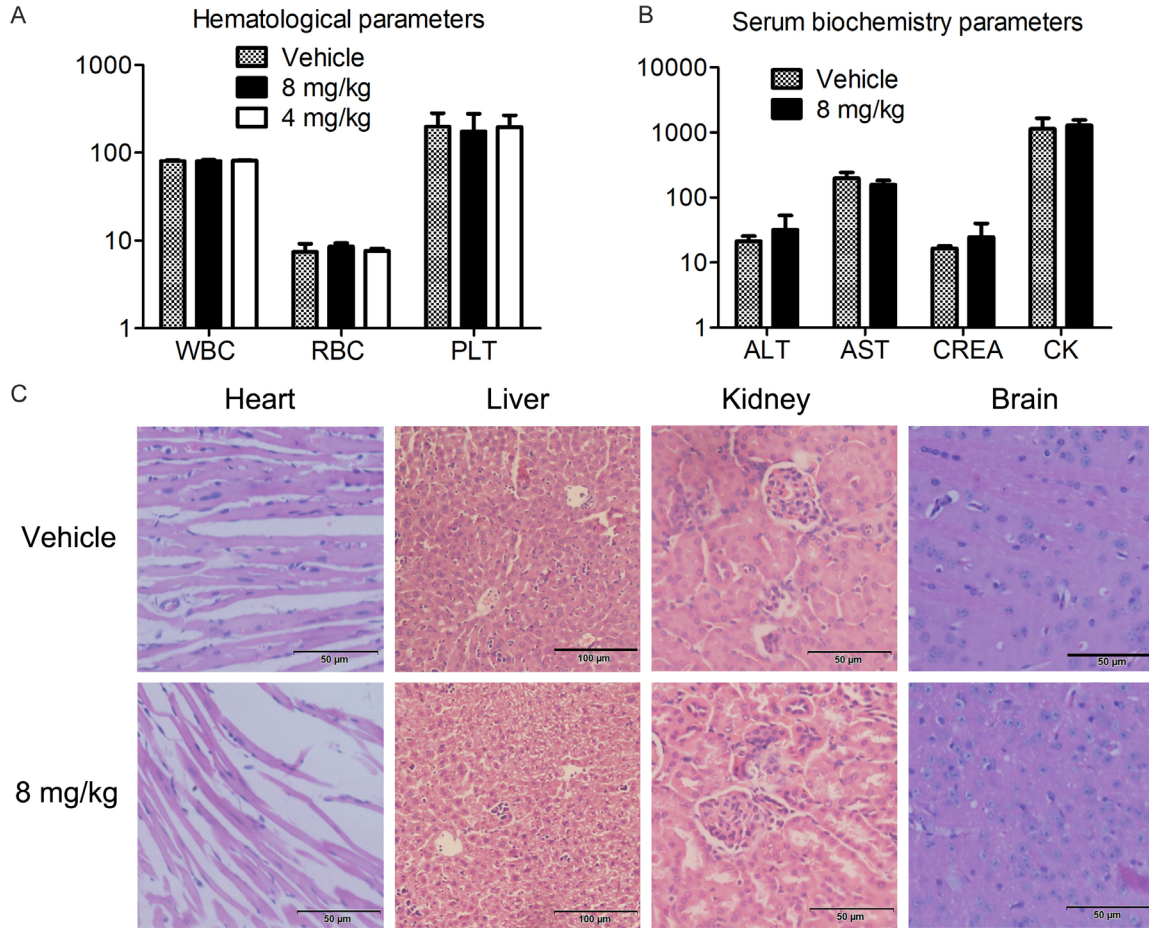
Figure 8. Flu didn't induce serious side effects in mice during the treatment. The mice in the 4T1 subcutaneous tumor model were sacrificed 17 days after the treatment. The main organs and blood of the mice were obtained for further analysis. Hematological and serum biochemistry analysis were performed after collecting eyeball blood of the mice. Heart, liver, kidney and brain of the mice were isolated and stained with H&E. (A and B) Flu treatment didn't cause significant changes in blood hematological (A) and serum biochemistry (B) parameters. The units of the parameters are shown as follows. WBC (white blood cell) and PLT (platelet), 10^9/L; RBC (red blood cell), 10^{12}/L; ALT (alanine transarninase), AST (aspartate aminotransferase) and CK (creatinine kinase), U/L; CREA(creatinine), uM. (C) Flu didn't cause obvious pathologic abnormalities in normal tissues of the mice. Images shown are representatives from each group. The scale bars represent 50 μm, 100 μm, 50 μm, 50 μm for heart, liver, kidney and brain, respectively.

obvious signs of pathological changes (**Figure 8C**).

Discussion

A major obstacle to successful breast cancer treatment is the metastasis to other organs of the body, including liver, bones, lungs and brain [5]. Brain metastasis is an end-stage disease of breast cancer progression, and its incidence increases with the application of advanced imaging techniques and the prolonged survival due to improvement of systemic disease treatment [5]. Traditional treatment options such as surgery, radiation, and chemotherapy showed

minimal efficacy, and the overall survival of these patients is on the order of months [5, 11]. Among the heterogeneous breast cancer subtypes, the incidence of brain metastases in patients with metastatic TNBC is approximately 40% and could be as high as 46%, depending on the cohorts [3, 6, 7, 11]. Many chemotherapy drugs used to treat primary TNBC can't cross the BBB, leading to therapeutic resistance. Therefore, finding new and effective drugs that could reach therapeutic concentrations in the brain is essential for improving the survival and quality of life of patients with brain metastatic TNBC [5, 34].

Antipsychotic drugs are easy to penetrate the BBB and lots of papers have reported their anticancer potentials [19-21]. This prompted us to investigate their potential to treat TNBC brain metastases. In the current study, we investigated the efficacy and mechanism of fluphenazine hydrochloride (Flu), an FDA-approved antipsychotic drug, to treat brain metastases of TNBC. Several publications have reported its anticancer abilities [21, 35]. Importantly, it has entered clinical trials for treating cancer (NCT00335647 and NCT00821301). The above information drives us to assess its potential to treat TNBC and brain metastasis. Our results showed Flu exhibited favorable antiproliferative efficacy in several TNBC cell lines as shown by MTT assay. This encourages us to further explore their anticancer potential and possible contribution mechanisms. We found that inducing G0/G1 cell cycle arrest and mitochondria-mediated intrinsic apoptosis contributed to Flu's anti-TNBC activities.

An uncontrolled, abnormal cell cycle is one of the hallmarks of cancer [36]. Disrupting cell cycle can suppress tumour growth and ultimately lead to apoptosis, contributing to cancer therapy [37]. Three drugs that target abnormal cell cycle have been approved by FDA to treat breast cancer [38-40]. Many more of such agents are in preclinical and clinical evaluation for cancer treatment, suggesting this is a promising strategy to cure cancer [41-44].

Numerous proteins are involved in precise cell cycle regulation when cells divide. Among them, many cyclin and cyclin-dependent kinase complex are important cell cycle regulators [45]. Cyclin D can bind to CDK4 and CDK6 and then promote E2F-dependent transcription followed by series of subsequent events that accelerate DNA replication and up-regulation of cyclin E and CDK2. The cyclin E/CDK2 positive feedback loop could phosphorylate Rb, thereby driving cancer cells through the G1/S checkpoint. p21 and p27 are two important negative regulators in G1/S cell cycle transition. They exert the inhibitory effects via inactivating the cyclin-CDK complexes [45, 46]. In the present study, Flu induced G0/G1 arrest in TNBC cells. Mechanistically, the expression levels of CDK2, CDK4, cyclin D1 and cyclin E are all down-regulated after Flu treatment. In addition, the expression of p21 and p27 are increased in MDA-MB-231 cells after Flu treatment. These data suggested that Flu induced G0/G1 cell cycle arrest via disrupting the corresponding cyclin-CDK complexes.

Cell cycle arrest can lead to programmed apoptosis [47]. There are two main apoptosis pathways. During the extrinsic apoptosis, caspase 8 is activated after the ligands interacting with the respective death receptors, after which caspase 3 and other downstream regulators are activated, leading to the apoptotic cascades [25, 48]. The other one is mitochondria-mediated intrinsic apoptosis, during which mitochondrial membrane integrity is damaged upon receiving the death signal. Then, cytochrome c is released from the mitochondria into the cytoplasm. Finally, caspase 9 is activated to cleave caspase 3 and initiate apoptosis [25, 48]. After Flu treatment, we observed ΔΨm loss in the cancer cells, indicating the damage of mitochondrial membrane integrity. Moreover, Z-LE(OMe)HD(OMe)-FMK (caspase-9 inhibitor) showed stronger activities than Z-LETD-FMK (caspase-8 inhibitor) to rescue Flu-induced apoptosis. ROS is mainly generated in the mitochondria during the electron transport process. Most tumor cells are under extremely high oxidative stress and therefore sensitive to the increased ROS [49]. In this study, the ROS levels in TNBC cells increased significantly after Flu treatment, which could impair the mitochondria membrane integrity. Besides, pretreatment with the antioxidant NAC partially rescued Flu-induced apoptosis. Numerous proteins are involved in regulating intrinsic apoptosis, among which Bax and Bcl-2 are two pivotal regulators [48]. We found that Flu treatment decreased the expression of anti-apoptotic Bcl-2 and increased the level of pro-apoptotic Bax. Taken together, these data implied that the mitochondria-mediated intrinsic pathway plays a more important role than the extrinsic pathway in Flu-induced apoptosis.

In vivo efficacy is an important parameter for assessing the anticancer potential of a drug. We established several different tumour models in the study. Before the treatment studies, we carried out a pharmacokinetic study to determine the concentration of Flu in the brain and in the circulation. Not surprisingly, Flu was highly distributed in the brain with a brain/plasma drug concentration ratio above 25 for at least 24 hours after administration. Then we evaluated the anticancer activities of Flu.

Notably, Flu suppressed the growth of both subcutaneous xenograft tumor and brain metastasis established by intra-carotid injection. Intracardiac, intracarotid and intracranial injection models are three main methods to established brain metastasis models [11]. Intracardiac injection will cause other metastases other than brain metastases, such as lung metastasis. Intracranial injection forgoes trans-BBB and extra-invasion process. That's why we chose intracarotid injection to establish the brain metastasis model in our study. Interestingly, the suppression rate of brain metastasis growth is more robust than that of the subcutaneous tumors, suggesting that the high penetration of Flu into the brain led to inhibition of brain metastasis growth. 4T1 cells extravasated into the mice brain within 7 days [50]. Thus, we also tried the strategy to start the treatment of 4T1 brain metastasis on day 8 postinoculation. Strikingly, Flu also suppressed the growth of brain metastasis with this treatment regimen. Lung, bone and liver metastasis are also major threats to the survival and quality of life of breast cancer patients [51]. Interestingly, Flu remarkably suppressed spontaneous lung metastasis of subcutaneous tumor, although it lacked inhibition of experimental bone metastasis and liver metastasis.

As an approved drug that has been in clinical use for a long time, the safety profiles of Flu are clear. This is the advantages to advance it into anti-cancer clinical trials. We investigated its safety profiles again. We evaluated the effects of different doses of Flu on the behavior of tumor-free mice. Then, we selected a 8 mg/kg/day dosage form by i.p. injection. This treatment regimen did not cause serious side effects in mice as indicated by toxicity evaluation. The exception is that Flu caused transient weight loss and extrapyramidal side effect (EPS). However, the EPS observed in a few cases disappeared within a few minutes, which can be prevented by using anti-Parkinson's disease drugs. In addition, the weight loss is reversible. The dose of 8 mg/kg/day in mice was converted to a human equivalent dose of 0.648 mg/kg/day when converted according to body surface area without changing the dosage form of the drug [52]. For a person weighting 60 kg, the dose is 38.88 mg. According to the drug label information of Flu from the US NIH (https://dailymed.nlm.nih.gov/dailymed/drugInfo.cfm?setid=0860b3f3-3116-40f8-bcb0-e5c-

47731bdc8), the total daily dosage of Flu for adult psychotic patients may range initially from 2.5 to 10 mg. However, daily doses up to 40 mg might be necessary for patients inadequately controlled, although controlled clinical studies have not been done to evaluate the safety of prolonged administration of such doses. Notably, the dosage form of Flu in the current study is different from that in patients. Flu dosage forms for use in patients include oral tablets, solutions for intramuscular or subcutaneous administration. Different dosage forms lead to different pharmacokinetic parameters [53]. Thus, the human equivalent dose of Flu might be different from 0.648 mg/kg/day. Moreover, if the dose of Flu in our study is really too high for human patients, we can improve drug delivery to the tumor site and reduce drug uptake in normal tissues through a variety of pharmacy optimizations [54], through which we are able to reduce the dose and systemic toxicity, while improving the treatment effect. A well-known example in the field of cancer treatment is the optimization of doxorubicin. Compared with free doxorubicin, pegylated liposomal doxorubicin (PLD, Doxil or Caelyx) uptake by normal tissues is lower, while drug concentrations in the tumor are enhanced. Thus, liposomal doxorubicin is with significantly reduced cardiotoxicity, a severe adverse effect may lead to congestive heart failure and death [55-57]. Therefore, we concluded that the relatively high dose of Flu in this study is not a barrier to repurpose it for the treatment of breast cancer with brain metastasis and lung metastasis.

However, the precise target and anticancer mechanism of Flu is not clear. Previous studies have shown different mechanisms of antipsychotic agents to fight against cancer, such us induction of autophagy, dysregulation of cholesterol homeostasis and disruption of lysosomal homeostasis [19, 20, 58]. Previous study had reported Flu inhibited acid sphingomyelinase. However, the direct anticancer target of Flu was still elusive. In this study, we observed a decrease in the expression levels of several proteins after Flu treatment, including some cyclins, CDKs and even total AKT and total ERK1/2. These may be caused by protein degradation or reduced gene transcription. Further research is still needed to validate these hypotheses. Next, we will study the changes in transcriptional activity after Flu treatment and investigate the effects of proteasome inhibitors

like MG132 on Flu-induced cell cycle arrest and apoptosis. Moreover, a combination of state-of-the-art technologies such as RNA-seq and mass spectrometry can be used to help elucidate the possible targets of Flu to inhibit breast cancer. Besides, we can optimize the chemical structure of Flu and synthesize more active compounds based on the target.

In summary, the encouraging results of our study laid the foundation for the repurposing of Flu to treat TNBC with brain and lung metastases, which currently lack any effective treatment options.

Acknowledgements

Disclosure of conflict of interest

None.

Abbreviations

TNBC, triple negative breast cancer; ER, estrogen receptor; PR, progesterone receptor; HER2, human epidermal growth factor receptor-2; BBB, blood-brain barrier; FCM, flow cytometry; CDK, cyclin-dependent kinase; $\Delta\Psi m$, mitochondrial membrane potential; ROS, reactive oxygen species; PI, propidium iodide; Rh123, rhodamine-123; NAC, N-acetyl-L-cysteine.

Address correspondence to: Luoting Yu, Department of Rehabilitation Medicine, State Key Laboratory of Biotherapy and Cancer Center, West China Hospital, Sichuan University and Collaborative Innovation Center for Biotherapy, 17#3rd Section, Ren Min South Road, Chengdu 610041, China. Tel: +86-28-85503817; Fax: +86-28-85164060; E-mail: yuluot@scu.edu.cn

References

[1] Desantis CE, Ma J, Goding Sauer A, Newman LA and Jemal A. Breast cancer statistics, 2017, racial disparity in mortality by state. Ca Cancer J Clin 2017; 67: 439-448.

[2] Rivenbark AG, O'Connor SM and Coleman WB. Molecular and cellular heterogeneity in breast cancer: challenges for personalized medicine. Am J Pathol 2013; 183: 1113-1124.

[3] Voduc KD, Nielsen TO, Perou CM, Harrell JC, Fan C, Kennecke H, Minn AJ, Cryns VL and Cheang MC. αB-crystallin expression in breast cancer is associated with brain metastasis. NPJ Breast Cancer 2015; 1.

[4] Mehlen P and Puisieux A. Metastasis: a question of life or death. Nat Rev Cancer 2006; 6: 449-458.

[5] Shah N, Mohammad AS, Saralkar P, Sprowls SA, Vickers SD, John D, Tallman RM, Luckewold B, Jarrell KE and Pinti M. Investigational chemotherapy and novel pharmacokinetic mechanisms for the treatment of breast cancer brain metastases. Pharmacol Res 2018; 132: 47-68.

[6] Arslan UY, Oksuzoglu B, Aksoy S, Harputluoglu H, Turker I, Ozisik Y, Dizdar O, Altundag K, Alkis N and Zengin N. Breast cancer subtypes and outcomes of central nervous system metastases. Breast 2011; 20: 562-567.

[7] Lin NU, Claus E, Sohl J, Razzak AR, Arnaout A and Winer EP. Sites of distant recurrence and clinical outcomes in patients with metastatic triple-negative breast cancer. Cancer 2008; 113: 2638-2645.

[8] Sawaya R. Considerations in the diagnosis and management of brain metastases. Oncology 2001; 15: 1163-1165.

[9] Malin D, Strekalova E, Petrovic V, Deal AM, Al AA, Adamo B, Miller CR, Ugolkov A, Livasy C and Fritchie K. αB-crystallin: a novel regulator of breast cancer metastasis to the brain. Clin Cancer Res 2014; 20: 56-67.

[10] Lin NU, Bellon JR and Winer EP. CNS metastases in breast cancer. J Clin Oncol 2006; 4: 3608-3617.

[11] Kodack David P, Askoxylakis V, Ferraro Gino B, Dai F and Jain Rakesh K. Emerging strategies for treating brain metastases from breast cancer. Cancer Cell 2015; 27: 163-175.

[12] Deeken JF and Löscher W. The blood-brain barrier and cancer: transporters, treatment, and trojan horses. Clin Cancer Res 2007; 13: 1663-1674.

[13] Basso J, Miranda A, Sousa J, Pais A and Vitorino C. Repurposing drugs for glioblastoma: from bench to bedside. Cancer Lett 2018; 428: 173-183.

[14] Dilly SJ, Clark AJ, Marsh A, Mitchell DA, Cain R, Fishwick CWG and Taylor PC. A chemical genomics approach to drug reprofiling in oncology: Antipsychotic drug risperidone as a potential adenocarcinoma treatment. Cancer Lett 2017; 393: 16-21.

[15] Turanli B, Grøtli M, Boren J, Nielsen J, Uhlen M, Arga KY, Mardinoglu A. Drug repositioning for effective prostate cancer treatment. Front Physiol 2018; 9: 500.

[16] Gupta SC, Sung B, Prasad S, Webb LJ, Aggarwal BB. Cancer drug discovery by repurposing:

teaching new tricks to old dogs. Trends in Pharmacol Sci 2013; 34: 508-517.

[17] Dalton SO, Johansen C, Poulsen AH, Nørgaard M, Sørensen HT, McLaughlin JK, Mortensen PB, Friis S. Cancer risk among users of neuroleptic medication: a population-based cohort study. Br J Cancer 2006; 95: 934-939.

[18] Mortensen PB. Neuroleptic treatment and other factors modifying cancer risk in schizophrenic patients. Acta Psychiat Scand 1987; 75: 585-590.

[19] Zong D, Zielinskachomej K, Juntti T, Mörk B, Lewensohn R, Hååg P and Viktorsson K. Harnessing the lysosome-dependent antitumor activity of phenothiazines in human small cell lung cancer. Cell Death Dis 2014; 5: e1111.

[20] Shin SY, Lee KS, Choi YK, Lim HJ, Lee HG, Lim Y and Lee YH. The antipsychotic agent chlorpromazine induces autophagic cell death by inhibiting the Akt/mTOR pathway in human U-87MG glioma cells. Carcinogenesis 2013; 34: 2080-2089.

[21] Klutzny S, Lesche R, Keck M, Kaulfuss S, Schlicker A, Christian S, Sperl C, Neuhaus R, Mowat J and Steckel M. Functional inhibition of acid sphingomyelinase by Fluphenazine triggers hypoxia-specific tumor cell death. Cell Death Dis 2017; 8: e2709.

[22] Hilf R, Bell C, Goldenberg H and Michel I. Effect of fluphenazine HCl on R3230AC mammary carcinoma and mammary glands of the rat. Cancer Res 1971; 31: 1111-1117.

[23] Syn NL, Lim PL, Kong LR, Wang L, Wong AL, Lim CM, Tks L, Siemeister G, Goh BC and Hsieh WS. Pan-CDK inhibition augments cisplatin lethality in nasopharyngeal carcinoma cell lines and xenograft models. Signal Transduct Target Ther 2018; 3: 9.

[24] Sun X, Zhan L, Chen Y, Wang G, He L, Wang Q, Zhou F, Yang F, Wu J and Wu Y. Increased mtDNA copy number promotes cancer progression by enhancing mitochondrial oxidative phosphorylation in microsatellite-stable colorectal cancer. Signal Transduct Target Ther 2018; 3: 8.

[25] Xia Y, Lei Q, Zhu Y, Ye T, Wang N, Li G, Shi X, Liu Y, Shao B and Yin T. SKLB316, a novel small-molecule inhibitor of cell-cycle progression, induces G2/M phase arrest and apoptosis in vitro and inhibits tumor growth in vivo. Cancer Lett 2014; 355: 297-309.

[26] Berman AY, Manna S, Schwartz NS, Katz YE, Sun Y, Behrmann CA, Yu JJ, Plas DR, Alayev A and Holz MK. ERRα regulates the growth of triple-negative breast cancer cells via S6K1-dependent mechanism. Signal Transduct Target Ther 2017; 2.

[27] Ballard P, Yates JWT, Yang Z, Kim DW, Yang CH, Cantarini M, Pickup K, Jordan A, Hickey M and Grist M. Preclinical comparison of osimertinib with other EGFR-TKIs in EGFR-Mutant NSCLC brain metastases models, and early evidence of clinical brain metastases activity. Clin Cancer Res 2016; 22: 5130-5140.

[28] Zhang S, Huang WC, Zhang L, Zhang C, Lowery FJ, Ding Z, Guo H, Wang H, Huang S and Sahin AA. Src family kinases as novel therapeutic targets to treat breast cancer brain metastases. Cancer Res 2013; 73: 5764-5774.

[29] Ye T, Xiong Y, Yan Y, Xia Y, Song X, Liu L, Li D, Wang N, Zhang L and Zhu Y. The anthelmintic drug niclosamide induces apoptosis, impairs metastasis and reduces immunosuppressive cells in breast cancer model. PLoS One 2014; 9: e85887.

[30] Oshima G, Stack ME, Wightman SC, Bryan D, Poli E, Xue L, Skowron KB, Uppal A, Pitroda SP and Huang X. Advanced animal model of colorectal metastasis in liver: imaging techniques and properties of metastatic clones. J Vis Exp 2016; e54657.

[31] Campbell JP, Merkel AR, Masood-Campbell SK, Elefteriou F and Sterling JA. Models of bone metastasis. J Vis Exp 2012; e4260.

[32] Xia Y, Song X, Li D, Ye T, Xu Y, Lin H, Meng N, Li G, Deng S and Zhang S. YLT192, a Novel, orally active bioavailable inhibitor of VEGFR2 signaling with potent antiangiogenic activity and antitumor efficacy in preclinical models. Sci Rep 2014; 4: 6031.

[33] Ranjan A, Gupta P and Srivastava SK. Penfluridol: an antipsychotic agent suppresses metastatic tumor growth in triple negative breast cancer by inhibiting integrin signaling axis. Cancer Res 2015; 76: 877-890.

[34] Lockman PR, Mittapalli RK, Taskar KS, Rudraraju V, Gril B, Bohn KA, Adkins CE, Roberts A, Thorsheim HR and Gaasch JA. Heterogeneous Blood-tumor barrier permeability determines drug efficacy in experimental brain metastases of breast cancer. Clin Cancer Res 2010; 16: 5664-5678.

[35] Jiang XW, Lu WQ, Shen XY, Wang Q, Lv J, Liu MY, Cheng FX, Zhao ZM and Pang XF. Repurposing sertraline sensitizes non-small cell lung cancer cells to erlotinib by inducing autophagy. JCI Insight 2018; 3.

[36] Hanahan D and Weinberg RA. Hallmarks of cancer: the next generation. Cell 2011; 144: 646-674.

[37] Evan GI and Vousden KH. Proliferation, cell cycle and apoptosis in cancer. Nature 2001; 411: 342-348.

[38] Finn RS, Crown JP, Lang I, Boer K, Bondarenko IM, Kulyk SO, Ettl J, Patel R, Pinter T and Schmidt M. The cyclin-dependent kinase 4/6 inhibitor palbociclib in combination with letrozole versus letrozole alone as first-line treat-

ment of oestrogen receptor-positive, HER2-negative, advanced breast cancer (PALOMA-1/TRIO-18): a randomised phase 2 study. Lancet Oncol 2015; 16: 25-35.

[39] Hortobagyi GN, Stemmer SM, Burris HA, Yap YS, Sonke GS, Paluchshimon S, Campone M, Blackwell KL, André F and Winer EP. Ribociclib as first-line therapy for hr-positive, advanced breast cancer. N Engl J Med 2016; 375: 1738-1748.

[40] Jr SG, Toi M, Neven P, Sohn J, Inoue K, Pivot X, Burdaeva O, Okera M, Masuda N and Kaufman PA. MONARCH 2: abemaciclib in combination with fulvestrant in women with HR+/HER2- advanced breast cancer who had progressed while receiving endocrine therapy. J Clin Oncol 2017; 35: 2875-2884.

[41] Lu CH, Chen SH, Chang YS, Liu YW, Wu JY, Lim YP, Yu HI and Lee YR. Honokiol, a potential therapeutic agent, induces cell cycle arrest and program cell death in vitro and in vivo in human thyroid cancer cells. Pharmacol Res 2017; 115: 288-298.

[42] Tian QT, Ding CY, Song SS, Wang YQ, Zhang A and Miao ZH. New tanshinone I derivatives S222 and S439 similarly inhibit topoisomerase I/II but reveal different p53-dependency in inducing G2/M arrest and apoptosis. Biochem Pharmacol 2018; 154: 255-264.

[43] Yue M, Li S, Yan G, Li C and Kang Z. Paeoniflorin inhibits cell growth and induces cell cycle arrest through inhibition of FoxM1 in colorectal cancer cells. Cell Cycle 2018; 17: 1-10.

[44] Rocha Lima CMS, Roberts PJ, Priego VM, Divers SG, Thomas MB, Boccia R, Stabler K, Andrews E, Malik RK, Aljumaily R, Hamm JT, Chiu VK, Richards DA, Nikolinakos P, Hussein MA, Schuster SR, Hoyer RJ, Shapiro GI, Dragnev KH and Owonikoko TK. Trilaciclib (G1T28): a cyclin dependent kinase 4/6 inhibitor, in combination with etoposide and carboplatin (EP) for extensive stage small cell lung cancer (ES-SCLC) -Phase 1b results. J Clin Oncol 2017; 35: 8568-8568.

[45] Vermeulen K, Van Bockstaele DR and Berneman ZN. The cell cycle: a review of regulation, deregulation and therapeutic targets in cancer. Cell Prolif 2003; 36: 131-149.

[46] Lapenna S and Giordano A. Cell cycle kinases as therapeutic targets for cancer. Nat Rev Drug Disco 2009; 8: 547-566.

[47] Schwartz GK and Shah MA. Targeting the cell cycle: a new approach to cancer therapy. J Clin Oncol 2005; 23: 9408-9421.

[48] Fesik SW. Promoting apoptosis as a strategy for cancer drug discovery. Nat Rev Cancer 2005; 5: 876-885.

[49] Azad MB, Chen Y and Gibson SB. Regulation of autophagy by reactive oxygen species (ROS): implications for cancer progression and treatment. Antioxid Redox Sign 2009; 11: 777-790.

[50] Wu W, Ye H, Wan L, Han X, Wang G, Hu J, Tang M, Duan X, Fan Y, He S, Huang L, Pei H, Wang X, Li X, Xie C, Zhang R, Yuan Z, Mao Y, Wei Y and Chen L. Millepachine, a novel chalcone, induces G(2)/M arrest by inhibiting CDK1 activity and causing apoptosis via ROS-mitochondrial apoptotic pathway in human hepatocarcinoma cells in vitro and in vivo. Carcinogenesis 2013; 34: 1636-1643.

[51] Kennecke H, Yerushalmi R, Woods R, Cheang MC, Voduc D, Speers CH, Nielsen TO and Gelmon K. Metastatic behavior of breast cancer subtypes. J Clin Oncol 2010; 28: 3271-3277.

[52] Nair AB and Jacob S. A simple practice guide for dose conversion between animals and human. J Basic Clin Pharm 2016; 7: 27-31.

[53] Hernández RM, Gascón AR, Calvo MB, Caramella C, Conte U, Domínguez-Gil A and Pedraz JL. Influence of route of administration and dosage form in the pharmacokinetics and bioavailability of salbutamol. Eur J Drug Metab Ph 1997; 22: 145-150.

[54] Bruschi ML. Strategies to modify the drug release from pharmaceutical systems. Edited by Marcos Luciano Bruschi, Woodhead Publishing; 2015. pp. 15-28.

[55] Abraham SA, Waterhouse DN, Mayer LD, Cullis PR, Madden TD and Bally MB. The liposomal formulation of doxorubicin. Method Enzymol 2005; 391: 71-97.

[56] Yildirim Y, Gultekin E, Avci ME, Inal MM, Yunus S and Tinar S. Cardiac safety profile of pegylated liposomal doxorubicin reaching or exceeding lifetime cumulative doses of 550 mg/m 2 in patients with recurrent ovarian and peritoneal cancer. Int J Gynecol Cancer 2010; 18: 223-227.

[57] Gabizon A, Shmeeda H and Barenholz Y. Pharmacokinetics of pegylated liposomal Doxorubicin: review of animal and human studies. Clin Pharmacokinet 2003; 42: 419-436.

[58] Wu L, Liu YY, Li ZX, Zhao Q, Wang X, Yu Y, Wang YY, Wang YQ and Luo F. Anti-tumor effects of penfluridol through dysregulation of cholesterol homeostasis. Asian Pac J Cancer Prev 2014; 15: 489-494.

Table S1. Sources of antibodies used in this study.

Antibodies	Source	Cat#
Caspase 3	Cell Signaling Technology	9664s
Bax	BD Bioscience	610982
Bcl2	BD Bioscience	610538
P27	Cell Signaling Technology	3698s
P21	Wanlei Bio	CY5088
CDK4	Abcam	ab108357
CDK2	Cell Signaling Technology	2546p
β-actin	Zen bioscience	200068-8F10
Cyclin E	BD Bioscience	51-14596R
Cyclin D1	Cell Signaling Technology	2978
AKT	Cell Signaling Technology	4658s
P-AKT	Cell Signaling Technology	4060s
ERK 1/2	Cell Signaling Technology	4695s
p-ERK 1/2	Cell Signaling Technology	4370
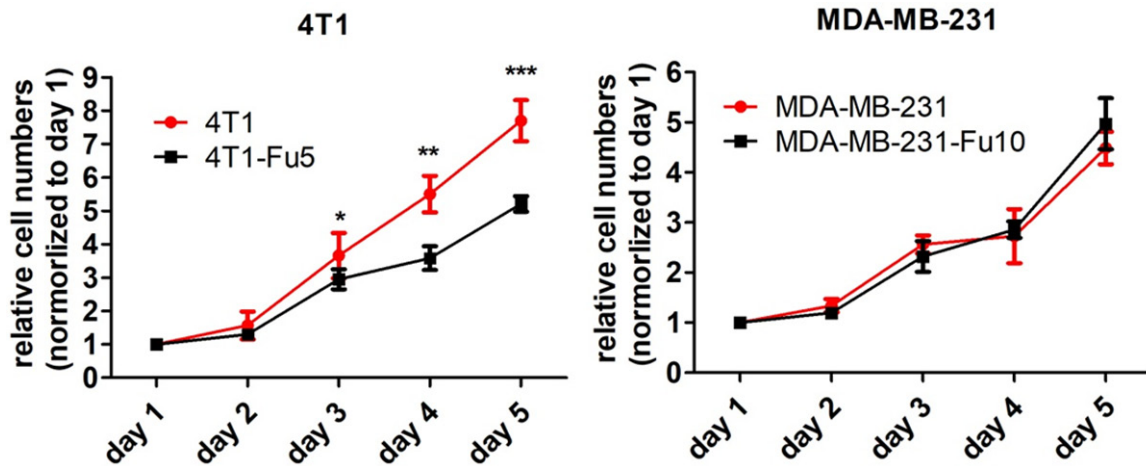
Figure S1. Proliferation curves of 4T1, 4T1-Fu5, MDA-MB-231 and MDA-MB-231-Fu10 cells. The above cells were seeded in 96-well plate at a density of 1500-3000 cells per well. Then cell numbers were measured by MTT for 5 consecutive days. Cell numbers were normalized based on the cell numbers on day 1, respectively (*$P<0.05$, **$P<0.01$, ***$P<0.001$).
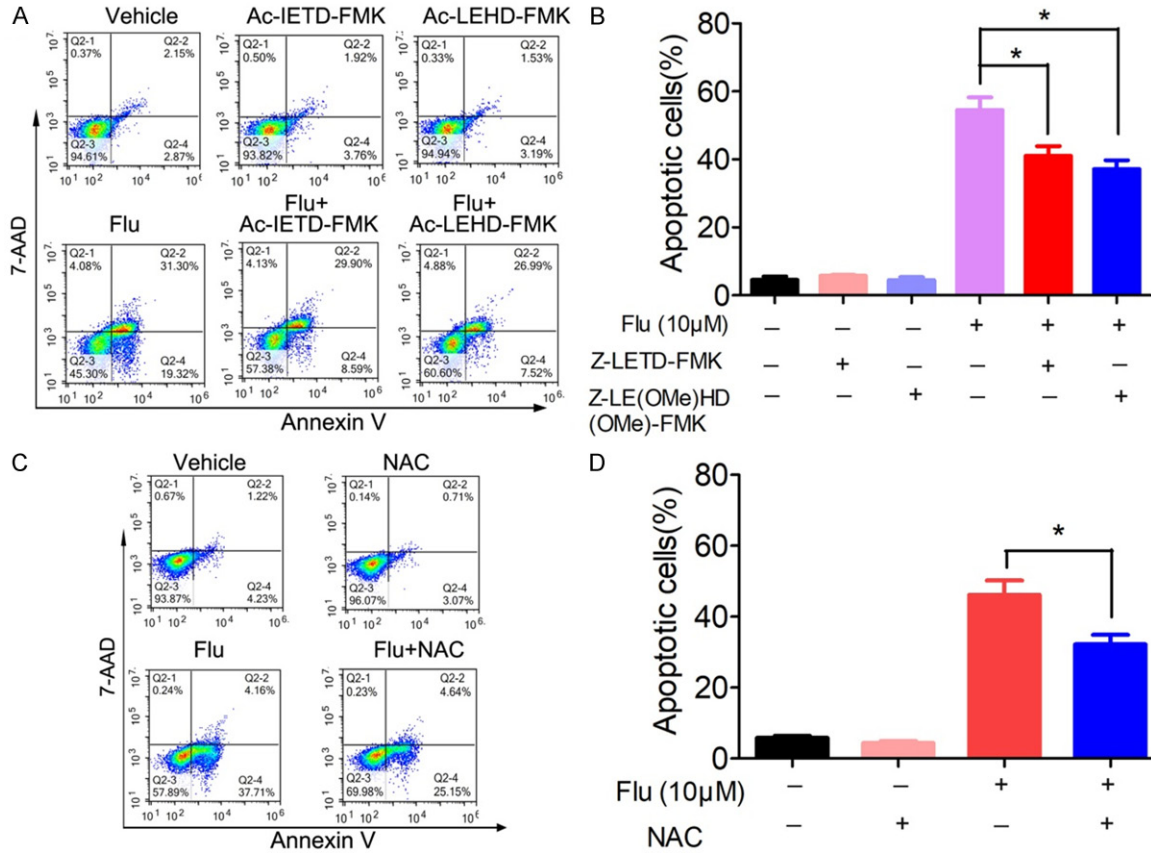
Figure S2. Effects of Flu on the intrinsic apoptosis pathway in MDA-MB-231 cells. (A and B) MDA-MB-231 cells were treated with 20 µM Flu alone or in combination with Z-LE(OMe)HD(OMe)-FMK (caspase-9 inhibitor) or in combination with Z-LETD-FMK (caspase-8 inhibitor) for 72 hours. Then the apoptosis of the cells were measured by FCM after AnnexinV-PE and 7-AAD labeling. (A) Images shown are representatives of three independent experiments. (B) Quantified values of the apoptosis. (C and D) MDA-MB-231 cells were pretreated with 2 mM NAC for 1 h and then treated with 20 µM Flu for 72 hours. The apoptosis of the cells were measured after AnnexinV-PE and 7-AAD labeling. (C) Images shown are representatives of three independent experiments. (D) Quantified values of the apoptosis. (*P<0.05; **P<0.01).
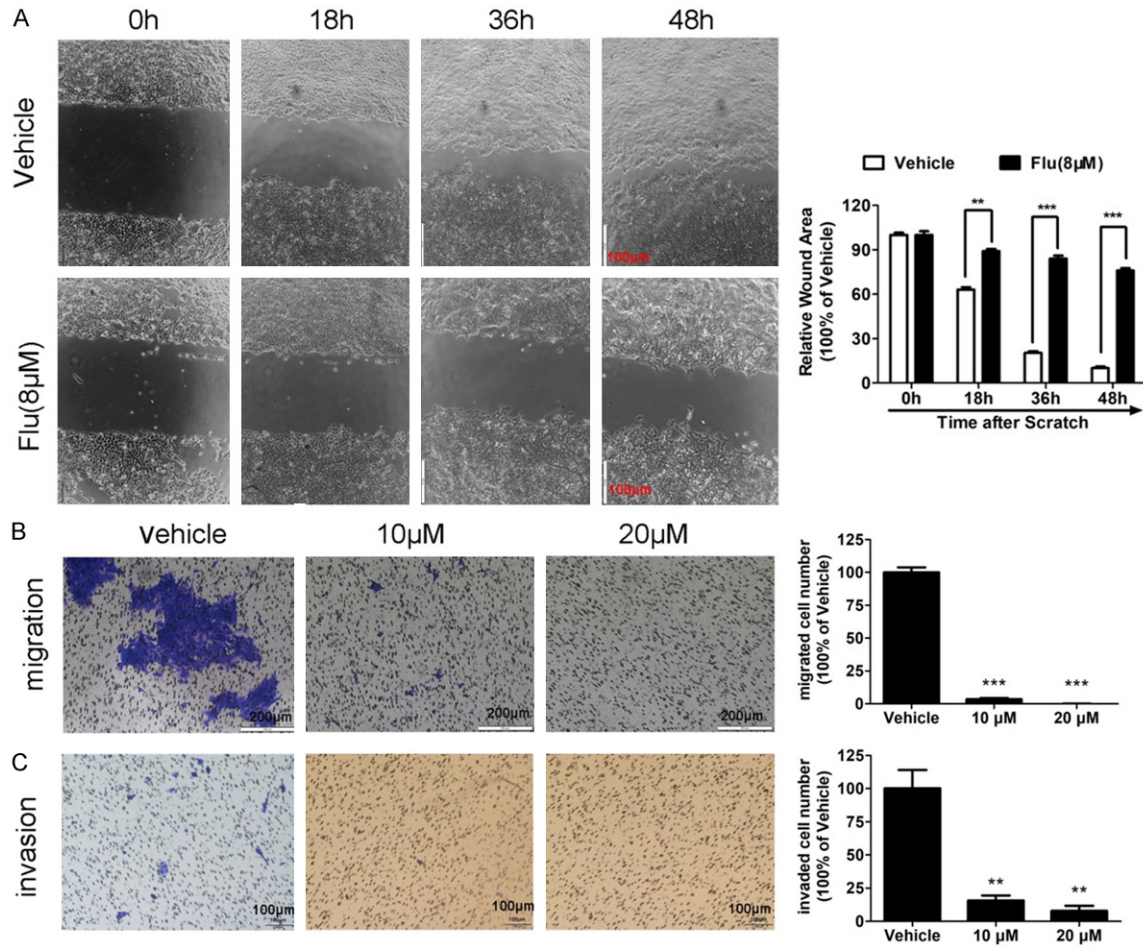
Figure S3. Flu suppresses cells migration and invasion *in vitro*. (A) Flu inhibited 4T1 cells migration in wound healing assay. Cells were scratched by 10 μL pipette when the cells grew to about 80% confluency and then treated with various concentrations of Flu. Cells' migration capacity was measured by photography. Wound width was measured manually. Quantified results are shown on the right (**P<0.01; ***P<0.001). (B) Flu inhibited 4T1 cell migration in the transwell migration assay. 5 × 10^4 4T1 cells were seeded in the top chamber of transwell in serum-free medium and treated with DMSO or indicated concentration of Flu. Regular medium with serum and equal amount of DMSO and Flu were added in the bottom chamber. Cells migrated through the membrane were stained and quantified. Quantified values are shown on the right (**P<0.01; ***P<0.001). (C) Flu inhibited 4T1 cell invasion in the transwell invasion assay. 10 × 10^4 4T1 cells were seeded in the top chamber of diluted Matrigel-coated transwell in serum-free medium and treated with DMSO or indicated concentration of Flu. Regular medium with serum and equal amount of DMSO and Flu were added in the bottom chamber. Cells invaded through the membrane were stained and quantified. Quantified values were shown on the right (**P<0.01; ***P<0.001).